THE EXPLOSIVE YIELDS PRODUCED BY THE FIRST GENERATION OF CORE COLLAPSE SUPERNOVAE AND THE CHEMICAL COMPOSITION OF EXTREMELY METAL POOR STARS

Alessandro Chieffi[1,2] and Marco Limongi[2]

1. Istituto di Astrofisica Spaziale e Fisica Cosmica (CNR), Via Fosso del Cavaliere, I-00133, Roma, Italy; achieffi@ias.rm.cnr.it

2. Istituto Nazionale di AstroFisica - Osservatorio Astronomico di Roma, Via Frascati 33, I-00040, Monteporzio Catone, Italy; marco@mporzio.astro.it

ABSTRACT

We present a detailed comparison between an extended set of elemental abundances observed in some of the most metal poor stars presently known and the ejecta produced by a generation of primordial core collapse supernovae. At variance with most of the analysis performed up to now (in which mainly the global trends with the overall metallicity are discussed), we think to be important (and complementary to the other approach) to fit the (available) chemical composition of specific stars. In particular we firstly discuss the differences among the five stars which form our initial database and define a "template" ultra metal poor star which is then compared to the theoretical predictions. Our main findings are as follows: a) the fit to [Si/Mg] and [Ca/Mg] of these very metal poor stars seems to favor the presence of a rather large C abundance at the end of the central He burning; in a classical scenario in which the border of the convective core is strictly determined by the Schwarzschild criterion, such a large C abundance would imply a rather low $^{12}C(\alpha,\gamma)^{16}O$ reaction rate; b) a low C abundance left by the central He burning would imply a low [Al/Mg] (< -1.2 dex) independently on the initial mass of the exploding star while a rather large C abundance would produce such a low [Al/Mg] only for the most massive stellar model; c) at variance with current beliefs that it is difficult to interpret the observed overabundance of [Co/Fe], we find that a mildly large C abundance in the He exhausted core (well within the present range of uncertainty) easily and naturally allows a very good fit to [Co/Fe]; d) our yields allow a reasonable fit to 8 out of the 11 available elemental abundances; e) within the present grid of models it is not possible to find a good match of the remaining three elements, Ti, Cr and Ni (even for an arbitrary choice of the mass cut); f) the adoption of other yields available in the literature does not improve the fit; g) since no mass in our grid provides a satisfactory fit to these three elements, even an arbitrary choice of the initial mass function would not improve their fit.

Subject headings: nuclear reactions, nucleosynthesis, abundances – stars: evolution – stars: interiors – stars: supernovae

1. Introduction

Extremely metal poor stars are among the oldest objects in our Galaxy and hence the analysis of their surface chemical composition provides us with invaluable information about the early chemical enrichment of the pristine material. Since these stars probably formed in an environment enriched by just the first generation of stars, they also constitute a unique

opportunity of observing directly the ejecta of a single stellar generation and not the complex superimposition of many generations of stars of different metallicity (as it happens when looking at stars of higher metallicity). Moreover, recent sets of observational data (McWilliam et al. 1995; Ryan, Norris & Beers 1996) have shown that below [Fe/H] $\simeq -2.5$ it exists a significative star to star scatter in the elemental abundances of many stars. This scatter has been interpreted (Audouze & Silk 1995) as a consequence of the fact that these stars formed in a highly inhomogeneous medium composed of substructures enriched by few supernovae (even one). Shigeyama & Tsujimoto (1998) and Nakamura et al. (1999) tried to interpret the chemical composition of the most metal poor stars in terms of a "single" supernova event. However, both attempts did not try to fit the surface composition of any of these metal poor stars but, instead, they adopted this scenario to try to reproduce the average trend with the metallicity of a few elemental ratios (i.e. [Cr/Fe], [Mn/Fe],[Co/Fe]). More recently, Argast et al. (2000) introduced a chemical evolution model able to resolve the formation of the initial chemical inhomogeneities and the following progressive homogenization but, also in this case, their main objective was to try to fit the observed spread of a few elements as a function of the iron abundance. We think it is time to test more thoroughly the idea that the most metal poor stars could have been formed by matter enriched by the ejecta of a single supernova event. In particular, by taking advantage of the fact that a rather large number of elemental abundances are available per each of these very metal poor stars, we think to be worth to directly compare these observed abundances to the ejecta of single primordial core collapse supernovae: the observational database we will analyze in this paper is formed by the five extremely metal poor stars (i.e. stars having [Fe/H] < -3.3) recently published by Norris, Ryan & Beers (2001). The outline of the paper is as follows: the observational database will be discussed in section 2 while the theoretical yields will be presented in section 3. Section 4 is devoted to the comparison between the observational and theoretical data. A final discussion and conclusion follows.

2. The observable

The most recent and homogeneous database of surface abundances of extremely metal poor stars available up to now is the one published by Norris, Ryan & Beers (2001) and consists of five stars of metallicity lower than [Fe/H]=-3.3. Three out of these five stars, i.e. CD$-38°245$ ([Fe/H]=-3.98), CS 22172-002 ([Fe/H]=-3.61) and CS 22885-096 ([Fe/H]=-3.66) show a remarkably similar pattern (panel a in Figure 1) with the exception of [C/Fe] which shows significative differences between CS 22172- 002 and CS 22885-096 (no C abundance is available for CD$-38°245$). Given the close similarity among these three stars it is meaningful to define an "average" (hereinafter AVG) star which represents all three of them. The
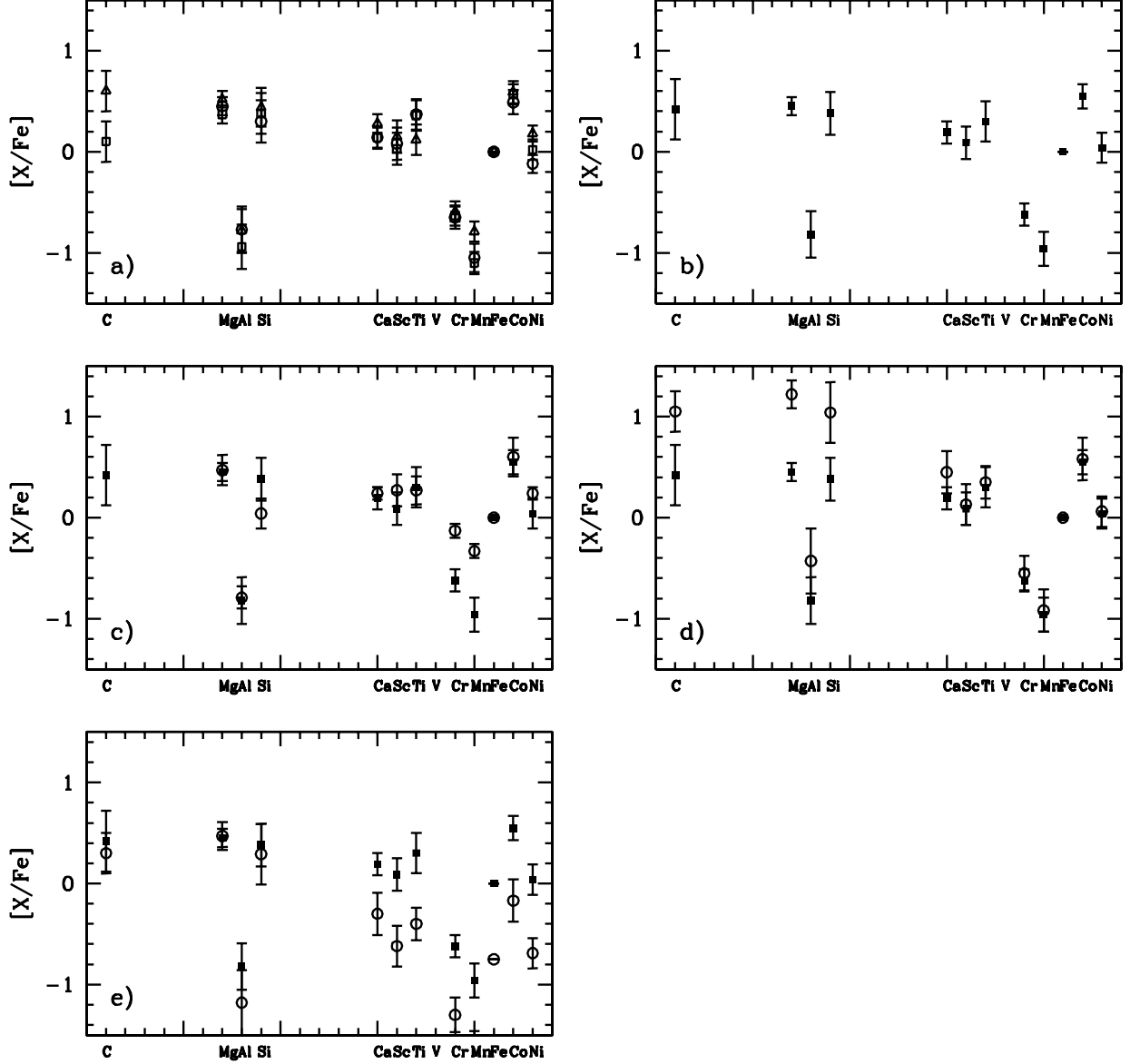
Fig. 1.— *Panel a):* elemental abundances of the three ultra metal poor stars CD − 38°245 ([Fe/H]=- 3.98) (*open circles*), CS 22172-002 ([Fe/H]=-3.61) (*open squares*) and CS 22885-096 ([Fe/H]=-3.66) (*open triangles*). *Panel b):* chemical pattern of the AVG star, which has been obtained by averaging the abundances of the elements shown in panel a). *Panel c):* comparison between CD − 24°17504 ([Fe/H]=-3.37) (*open circles*) and the AVG star (*filled squares*). *Panel d):* comparison between CS 22949-037 ([Fe/H]=- 3.79) (*open circles*) and the AVG star (*filled squares*). *Panel e):* same as panel d) but with the abundances of CS 22949-037 ([Fe/H]=- 3.79) (*open circles*) shifted downward by 0.7 dex.

chemical pattern of this AVG star is shown in panel b) of the same figure. The comparison between the AVG star and $CD - 24^{\circ}17504$ ([Fe/H]=-3.37) is shown in panel c). Also this star shows a chemical pattern which closely matches that of the other three stars with the exception of the elements Cr and Mn which are significantly more abundant (by a factor three to four) in $CD-24^{\circ}17504$ than in the other three stars. No C abundance determination is available for this star. Panel d) in the same figure shows the comparison between the AVG star and CS 22949-037 ([Fe/H]=- 3.79). While there is a clear agreement between this and the AVG star for the elements from Ca to Ni, the lighter ones appear to be, in this star, much more abundant (by a factor of five on the mean) than in the AVG star. This is clearly shown in panel e) where all the abundances of CS 22949-037 have been shifted downward by 0.7 dex: all the elements between C and Si now follow a pattern similar to the one shown by the AVG star. This star shows also an extremely high [N/Fe] ($\simeq$ 2.7 dex), value which is much larger than the factor of five required to fit the bulk of the elements up to Si. Leaving apart this last star which certainly shows significative differences respect to the other ones, we feel confident to say that the other four stars are similar enough to be well represented by the AVG star: therefore in the following we will consider this "template" star as the "observable" worth to be compared with the theoretical expectations.

3.   Theoretical yields

The theoretical yields we will adopt in the following analysis are based on a new set of zero metallicity massive stars ranging in mass between 15 and 80 $M_{\odot}$. These evolutions have been computed with the latest version of the FRANEC code (Chieffi, Limongi & Straniero 1998), rel. 4.84. This version of the code does not differ significantly from the one adopted by Limongi, Straniero & Chieffi (2000). Let us just remind that these stellar models have been evolved with a network including 179 isotopes fully coupled to the physical evolution of the stars from the pre main sequence until the central temperature reaches 6 10^9 K. A quantity which plays a major role in determining the final yields of most of the intermediate mass elements is the Carbon abundance left by the central He burning as largely discussed by, e.g., Weaver & Woosley, (1993) and Imbriani et al. (2001). This abundance is determined by the combined effects of the $^{12}C(\alpha, \gamma)^{16}O$ reaction rate and the behavior of the convective core during the latest part of the central He burning phase (Imbriani et al. 2001); however, in a classical scenario in which the border of the convective core is determined strictly by the Schwarzschild criterion, the final C abundance is mainly controlled by the adopted $^{12}C(\alpha, \gamma)^{16}O$ rate. In order to bracket the possible values for this rate we chose to compute two sets of models, one by adopting the rate published by Caughlan et al. (1985), hereinafter set H, and a second one with the rate given by Caughlan & Fowler (1988), hereinafter set

L. For sake of completeness Table 1 lists the C mass fraction X_C left by the He burning for all the masses in the two sets of models.

The explosive nucleosynthesis has been computed within the frame of the radiation dominated shock approximation (Weaver & Woosley, 1980; Arnett 1996). More specifically it is assumed that, as the shock wave (escaping the iron core with energy E) moves outward in mass through the massive star envelope, the pressure inside the shock front is nearly constant and dominated by the radiation pressure. Under this assumption each zone of the presupernova model is heated up to a temperature T_{shock} given by:

$$E_{expl} = \frac{4}{3}\pi R^3 a T_{shock}^4$$

where a is the Stefan-Boltzmann constant, E_{expl} is the explosion energy, T_{shock} and R are the temperature behind the shock and its location. The shock density can be easily derived by imposing the shock to be mildly strong, i.e.,

$$\rho_{shock} = f \cdot \rho_{pre-shock}$$

where $f = 4$. By the way let us underline that the final yields would not significantly change even assuming a strong shock ($f = 7$). The temporal variation of the temperature and density in each mass layer is obtained by assuming the matter to expand adiabatically ($T \propto \rho^{\gamma-1}$) at the escape velocity ($v = \sqrt{2GM/R}$) and the density to decline following an exponential low, i.e.:

$$\rho(t) = \rho_{shock} \cdot e^{-t/\tau}$$

where

$$\tau = \left(\frac{1}{\rho}\frac{\partial\rho}{\partial t}\right)^{-1} = \frac{R}{3v} = \frac{1}{\sqrt{24\pi G\rho}} = \frac{446}{\sqrt{\rho}}$$
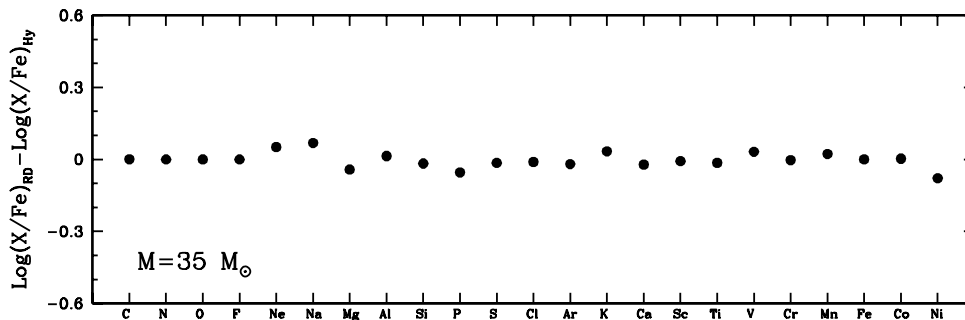

Fig. 2.— Comparison between the final explosive (X/Fe) computed with two different techniques: radiation dominated shock approximation versus hydro code.

In these computations (unless explicitly stated) we assume always a final explosion energy equal to 1.2×10^{51} erg (1.2 foe) and an initial collapse of all the mass zones outside the iron core over a time of 0.5 s (Thielemann, Nomoto & Hashimoto 1996). The chemical evolution has been followed by solving the same nuclear network adopted into the presupernova evolutions together to the temporal variation of temperature and density.

The elemental yields coming from set H have been already published by Limongi & Chieffi (2002), while the ones obtained for the set L are reported in Tables 2-7: for each mass we provide, as we usually do, the elemental yields in solar masses for different possible choices of the ^{56}Ni ejected (shown in the first row), after all unstable isotopes have been decayed into their stable form.

In addition to the full set of explosions computed within the frame of the radiation dominated shock approximation, we have also computed one explosion with an hydro code. In particular we computed the explosion of the $35M_\odot$ (set H). The hydro code solves the full hydrodynamical equations (included the gravitational field) in spherical symmetry and in lagrangean form together to the same nuclear network adopted into the presupernova evolutions. In this case the explosion has been induced by imposing the innermost edge of the envelope to move like a piston having an initial velocity V_0 and following a simple ballistic trajectory under the gravitational field of the compact remnant. The present version of this code does not take into account the time delay between collapse and explosion yet. The initial velocity V_0 has been tuned to obtain the ejection of 0.10 $M_\odot$ of ^{56}Ni: the corresponding final kinetic energy is 2.86 foes and the mass cut (i.e. the mass limit which separates the fraction of the star actually ejected in the interstellar medium from the fraction which remains locked in the remnant) is located at 2.37 $M_\odot$. Also the explosive yields computed with the radiation dominated shock approximation were obtained by imposing both the same kinetic energy at infinity and the ejection of 0.1 $M_\odot$ of ^{56}Ni. It is interesting to note that the mass coordinate which corresponds to this amount of ^{56}Ni, i.e. 2.36 $M_\odot$, is very close to the one obtained with the hydro code. Figure 2 shows that the two sets of yields are in excellent agreement, the differences remaining confined well within 0.1 dex. We computed other explosions on the same initial model for different final kinetic energies and found always a good agreement between the two techniques. The goodness of this comparison obtained for this specific model obviously does not guarantee that the same agreement holds for other masses. We plan to address this problem in a forthcoming paper.
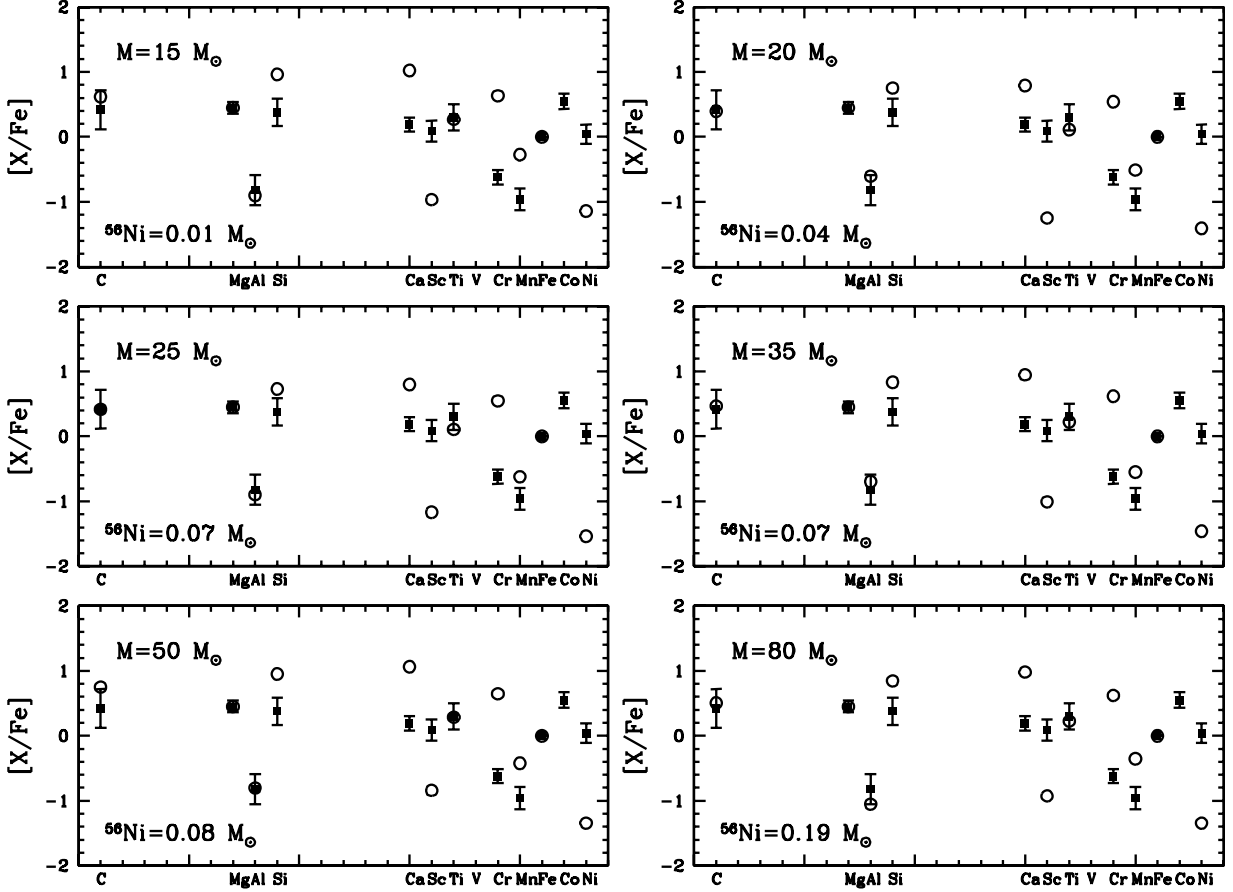
Fig. 3.— Comparison between the AVG star (*filled squares*) and the ejecta of the six masses in our grid (*open circles*). These models have been computed by adopting the $^{12}C(\alpha,\gamma)^{16}O$ reaction rate quoted by Caughlan et al. (1985). The ^{56}Ni shown in each panel is the one needed to fit the observed [Mg/Fe].

4. Fit to the AVG star

Let us discuss the fit to the AVG star under the hypothesis that its elemental ratios are the result of a single type II supernova event. The lack of a realistic description of the explosion of a core collapse supernova allows some freedom about the choice of the mass cut. Under the hypothesis that each cloud of pristine material is polluted by just a single supernova event, a possible way to choose the mass cut is simply that of imposing the fit to a given [X/Fe]. Since Mg is rather well measured and it is also produced sufficiently far from the center that it is not significantly affected by the precise location of the mass cut, we tentatively chose to fix the mass cut by imposing the fit to the observed [Mg/Fe]. It goes without saying that, since the yield of Mg varies with the initial mass, also the mass cut will vary with the mass of the star. The fit to the AVG star which is obtained with this choice for the mass cut is shown in Figure 3 (for the set H) and in Figure 4 (for the set L). Figure 3 shows that the fit to the two light elements C and Al (Mg is imposed) is remarkably good for all the six masses in our grid while it worsens progressively as one moves towards heavier nuclei. Neither Si nor Ca are fitted by any mass in our grid so as their internal ratio [Si/Ca]. The fit to the heaviest elements (Sc, Ti, Cr, Mn, Fe, Co and Ni), which are produced only by the complete and/or incomplete explosive Si burning, is even worst, with the exception of Ti which is very well fitted by all the models.

The fit to the AVG star with the set L (Figure 4) shows a better agreement because in this case both Si and Ca are very well reproduced by almost all stellar models. By the way, note that the 25 $M_\odot$ does not produce enough ^{56}Ni to fit the observed [Mg/Fe]; therefore in this case we simply fixed the mass cut at the border of the Fe core, choice which corresponds to the largest possible amount of ^{56}Ni. Conversely, [Al/Fe], which was fitted by all the masses of set H, now is fitted only by our most massive stellar model, i.e. the $80 M_\odot$. A detailed discussion of the dependence of the yields of the various elements on the carbon abundance left by the He burning may be found in Imbriani et al. (2001) and hence here we simply remind that Mg and Al scale directly with the Carbon abundance left by the He burning because are both direct products of the Carbon burning. The yields of Mg and Al produced by the two sets (H and L) of models are shown in the two upper panels of Figure 5, while the trend of [Al/Mg] with the initial mass for the two sets of models is shown in the lowest panel of the same figure. The value of [Al/Mg] for the AVG star (-1.27 dex) (solid horizontal line) as well as its error bar (dotted lines) are also shown in Figure 5, lowest panel. It is readily evident that while all the models of set H fall within the error bar of the observed [Al/Mg], most of the models of set L lie well above the range of compatibility. The adoption of set L changes also the fit to the heaviest elements (Sc through Ni) without leading anyway to an acceptable fit. More specifically: [Sc/Fe] remains systematically at least 1 dex below the observed value for all the masses in our grid, [Ti/Fe] (which was always well reproduced in
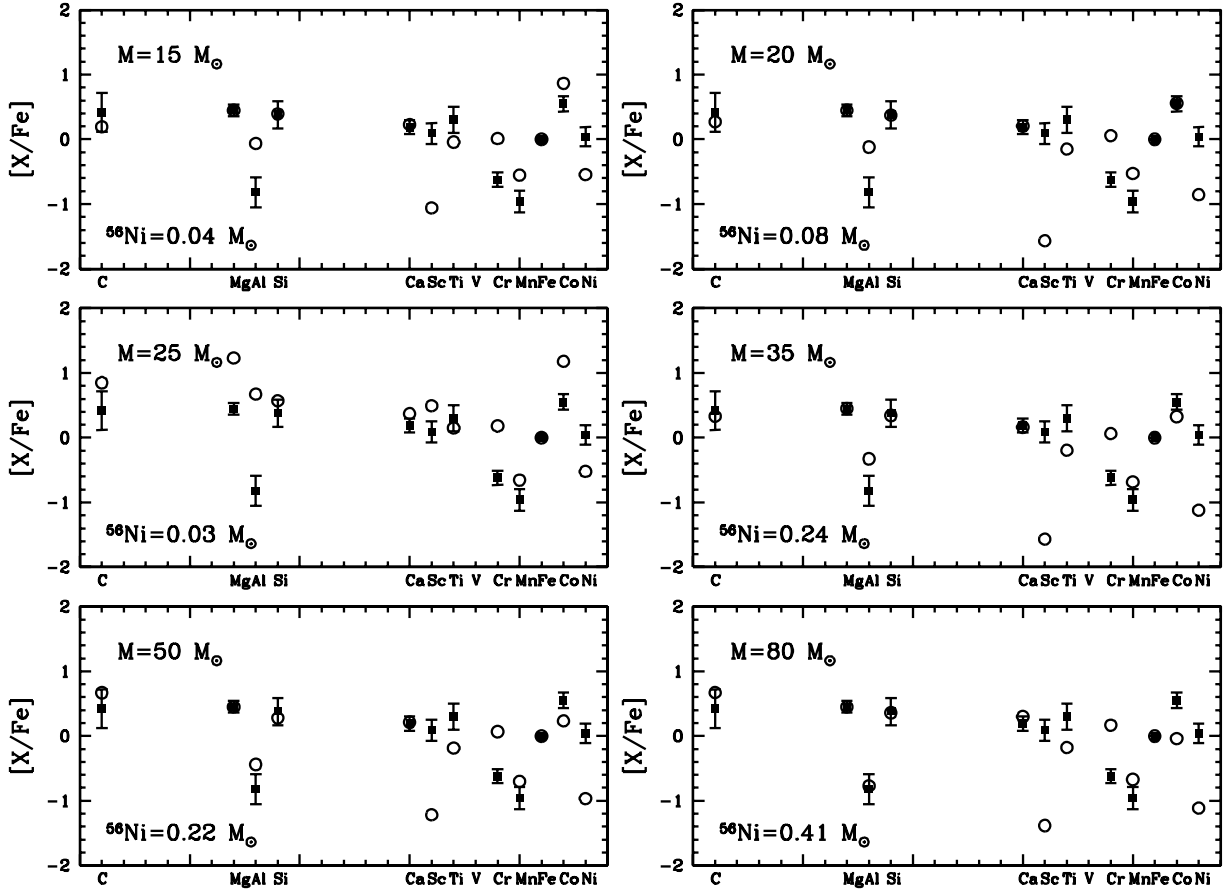
Fig. 4.— Same as Figure 3 but with models computed by adopting the $^{12}C(\alpha, \gamma)^{16}O$ reaction rate quoted by Caughlan & Fowler (1988).

the set H) is now underestimated by 0.4-0.6 dex, [Cr/Fe] and [Mn/Fe] are both overproduced (by 0.6 and 0.3 dex respectively) by all masses, [Co/Fe] shows a trend with the initial mass (in particular it lowers as the initial mass increases) and a good fit is obtained for a mass of the order of 20 $M_\odot$ while [Ni/Fe] is always underestimated by a factor ranging between 0.6 and 1 dex.

One could argue at this point that there is a contradiction between the present results and those reported by Imbriani et al. (2001) where it is stated that a low C abundance (i.e. set H) is necessary to preserve a scaled solar abundances. To clarify this apparent contrasting results, we show in Figure 6 a comparison between the [X/Mg] obtained with set L (open squares) and set H (filled squares), where each panel refers to a specific mass. The comparison refers to the elements which are not significantly affected by the mass cut (provided that the fall back is not exceedingly strong). The crosses mark the values obtained for the AVG star. Imbriani et al. (2001) computed the evolution of one star (the 25 $M_\odot$) of solar chemical composition and found (among other things) that: a) the abundances of the light elements (up to Al and excluding O) scale directly with the C abundance while the heaviest ones (up to Ca) scale inversely with C (see fig.16 in (Imbriani et al. 2001)) and b) if a 25 $M_\odot$ would be the main representative of a generation of massive stars, as suggested also by Weaver & Woosley, (1993), then a rather low C abundance should be preferred to keep the even intermediate mass elements (Mg to Ca) in roughly scaled solar proportions. All the panels in Figure 6 confirm point a), i.e. that [Si,S,Ar,Ca/Mg] scale inversely with the Carbon abundance left by the central He burning. Also point b) is well confirmed by the present computations since also in the case the 25 $M_\odot$ of set H gives a better scaled solar abundances for [Si,S,Ar,Ca/Mg] (see Figure 6) than set L. However, the new thing which comes out from these Z=0 models is that, for all the other masses in our grid, set L gives a much closer scaled solar distribution than set H does. If the 25 $M_\odot$ were not really representative of the ejecta provided by a generation of solar metallicity core collapse supernovae, also in that case probably a quite large C abundance at the end of the central He burning should be preferred. In the following, since set L provides a much better fit to both [Si/Mg] and [Ca/Mg] than set H does for most of the masses in our grid, we will further analyze only models computed with the rate quoted by Caughlan & Fowler (1988) for the $^{12}C(\alpha, \gamma)^{16}O$.

All the elements between Sc and Ni are produced by either the incomplete and/or the complete explosive Si burning in the deepest layers of the star, and hence they are those which are most affected by the adopted mass cut. Hence, the lack of a good fit to these elements could be simply due to a wrong choice of the mass cut. In order to show more clearly how the predicted [X/Fe] match the corresponding observed values, it is useful to introduce a new abundance ratio: $\{X/Fe\}_{star}$. This is simply $Log(X_{model}/Fe_{model}) - Log(X_{star}/Fe_{star})$,

i.e. the difference between the predicted and the observed ratio. This ratio differs from the classical "[X/Fe]" simply because in this case the "reference" star is not the Sun but the star to be fitted. The name *star* on the lower right corner of this parameter clearly identifies the "reference star" adopted to compute that specific ratio. This is a useful parameter because it readily shows the goodness of a fit (obviously $\{X/Fe\}_{star} = 0$ means a perfect fit of that star). Figure 7 shows how $\{Cr, Mn, Sc, Ti, Co, Ni/Fe\}_{AVG}$ vary with the amount of ^{56}Ni ejected (i.e. their dependence on the mass cut) for each specific mass. The panels referring to Ti, Ni, and Cr clearly show that there is no hope to obtain a good fit to the AVG star for any value of the mass cut, while those referring to the other three elements (Sc, Co and Mn), show that (at least for the 20, 35 and 50 $M_\odot$) it exists a value of ^{56}Ni which would allow the simultaneous fit to these three elements. Unfortunately this ^{56}Ni abundance is larger than that required to fit [Mg/Fe] and hence the fit to the light elements worsens somewhat. The best overall fits to the block of available elements is shown in Figure 8. The closest match to the AVG star is obtained with the ejecta of the 35 and 50 $M_\odot$.

The systematic lack of a good fit to Cr, Ti and Ni clearly indicates that something crucial has been missed in the computation of the yields. Though a detailed exploration of all the possible causes for such lack of fit is beyond the scope of the present paper, we made some tests by varying both the energy of the shock (between 1 and 3 foes) and the time delay (between 0 and 1 sec) without improving appreciably the fits shown above.

Alternative yields for zero metal massive stars have been published by Woosley & Weaver (1995), hereinafter WW95, and Umeda & Nomoto (2002), hereinafter UN02. None of the two papers provides yields as a function of the ^{56}Ni ejected and hence there is no way to impose the fit to any of the [X/Fe]. Figure 9 shows, for the four masses 15, 20, 25 and 30 $M_\odot$, the fits obtained by adopting the UN02 yields. The first thing worth noting is that none of the four masses provides an overall good fit to the data. Zooming in the various panels, Si and Ca are always rather well fitted (occurrence which should indicate a rather high C abundance) while the lighter elements are fitted only in the mass range 20-25 $M_\odot$. [Al/Mg] shows a behavior exactly opposite to ours: while we find that [Al/Mg] lowers as the initial mass of the star increases, UN02 find that this ratio increases with the mass of the star. Also these yields do not allow the fit to Ti, Cr and Ni for any mass in the available range: even more intriguing is the fact that the discrepancies are qualitatively very similar to the one we obtain with our yields: in particular, also these yields show that [Ti/Fe] and [Ni/Fe] are systematically underproduced with respect to the observed value for all the masses, while [Cr/Fe] is always overproduced by the models. The last two elements, Sc and Co, are heavily underproduced by all the UN02 models while Mn is well fitted by the two more massive models.
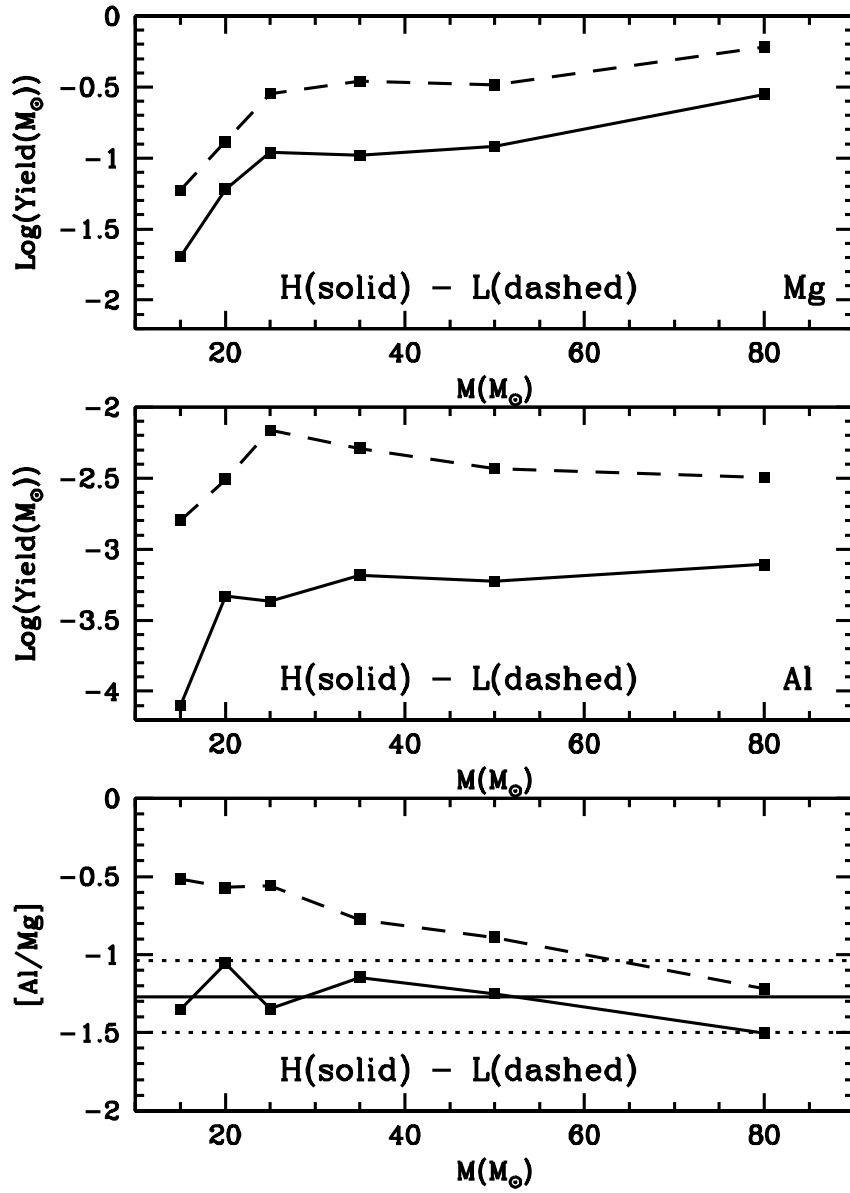
Fig. 5.— *Upper panel*: yield of Mg as a function of the initial mass for both set L (solid line) and set H (dashed line). *Middle panel*: same as the upper panel but for Al. *Lower panel*: [Al/Mg] as a function of the initial mass for both set L (solid line) and set H (dashed line). The solid and dotted horizontal lines mark the [Al/Mg] value and the error bar of the AVG star.
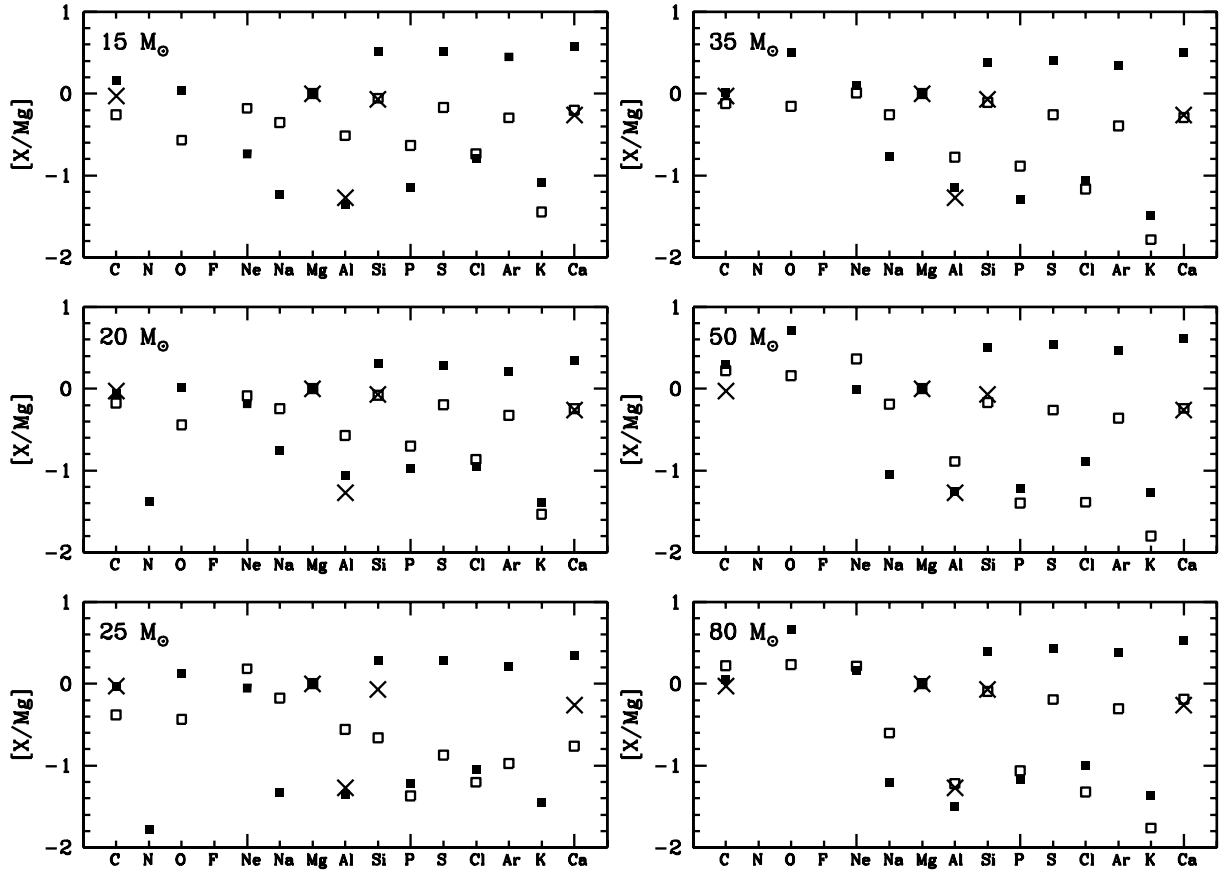
Fig. 6.— Comparison between the [X/Mg] obtained for set L (open squares) and set H (filled squares). The crosses mark the values obtained for the AVG star. Each panel refers to a specific mass.
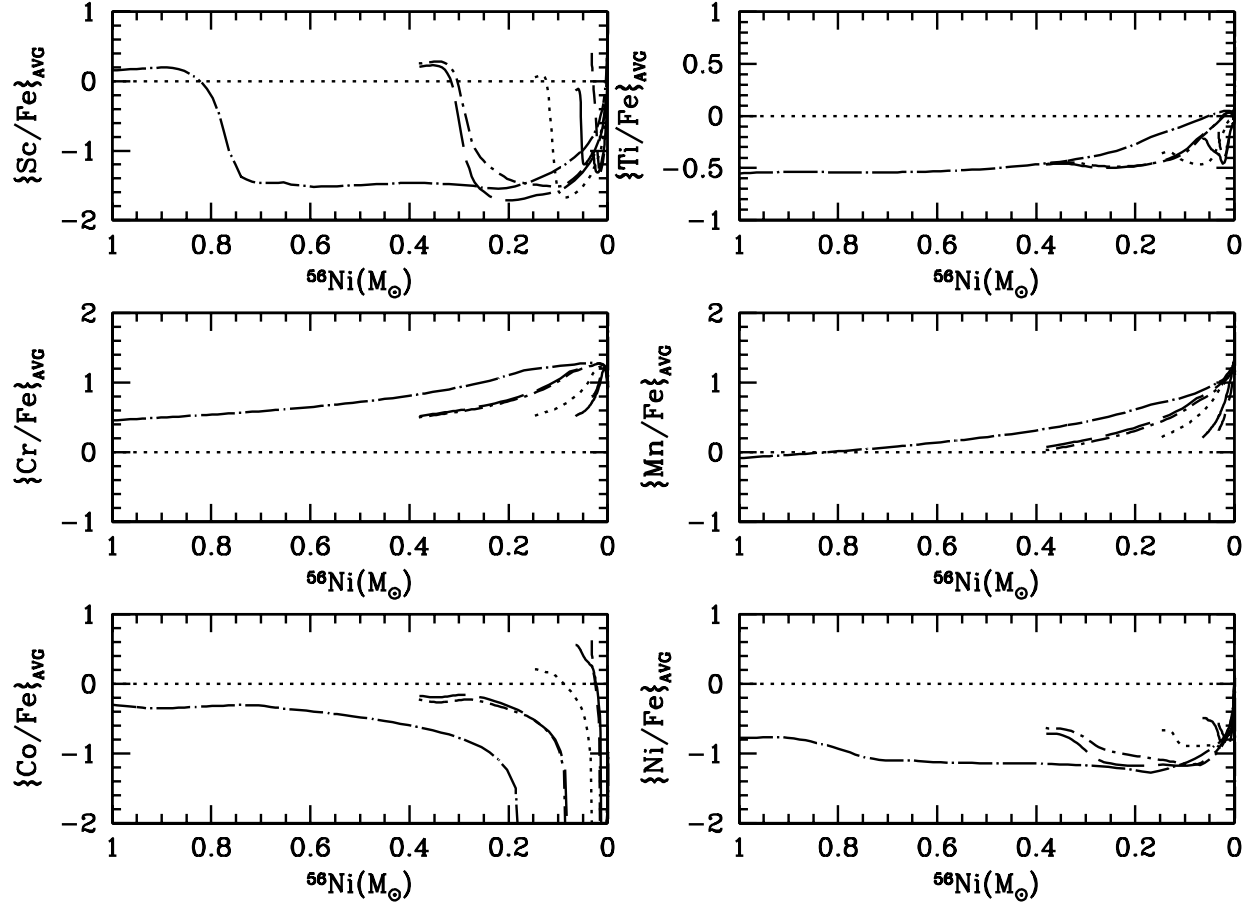
Fig. 7.— Trends of the [Sc,Ti,Cr,Mn,Co,Ni/Fe], i.e. elements produced by the complete and incomplete explosive Si burning, with the amount of Fe ejected. The six lines in each panel refer to: 15M$_\odot$ (*solid*), 20M$_\odot$ (*dotted*), 25M$_\odot$ (*short dashed*), 35M$_\odot$ (*long dashed*), 50M$_\odot$ (*dot short dashed*), 80M$_\odot$ (*dot long dashed*).
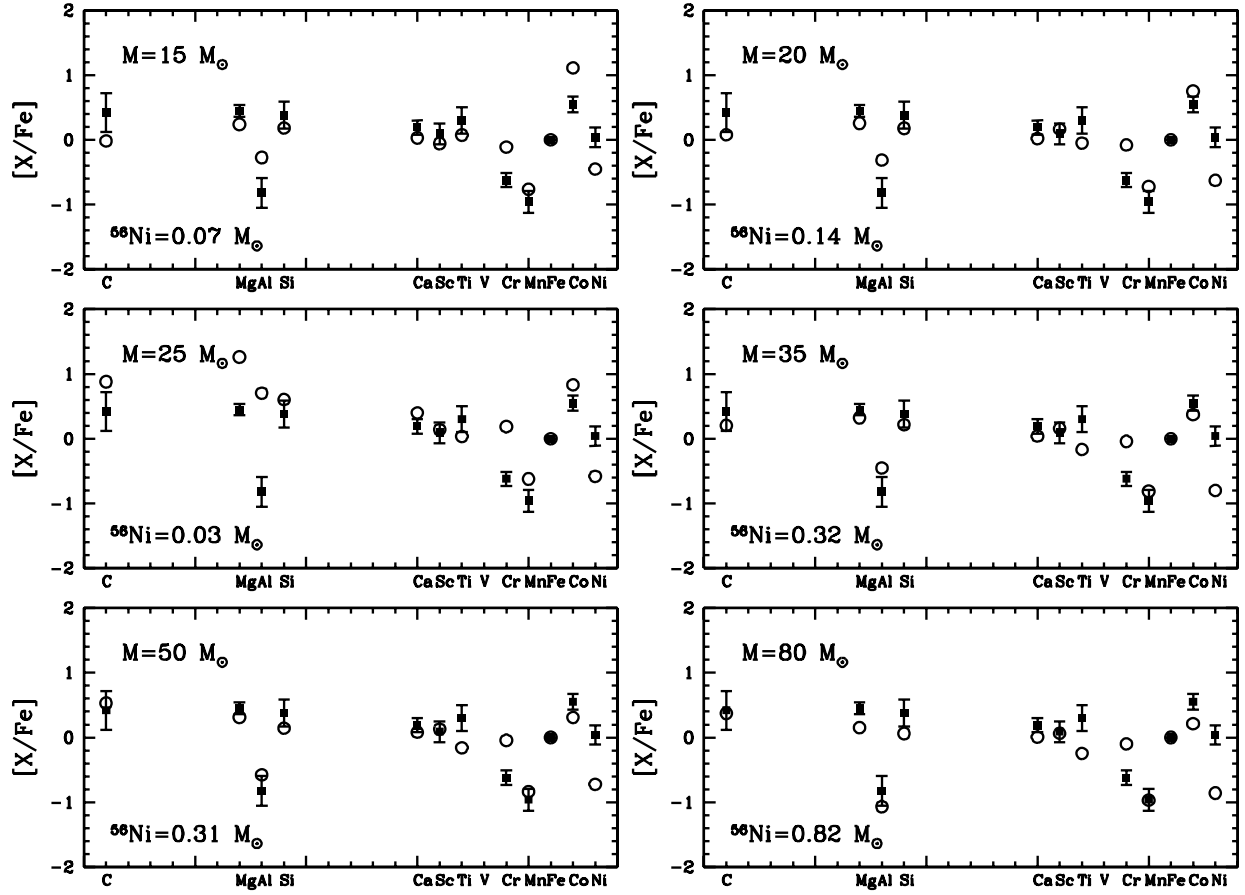
Fig. 8.— Same as figure 4 but with a choice of the mass cut which minimizes the overall differences between the AVG star and the theoretical values.

Figure 10 shows the fit to the AVG star with the yields provided by WW95. The grid is now formed by a 15, 25, 30 and 35 $M_\odot$. Also in this case none of the models reproduces the data. The element C to Ca are systematically underproduced with respect to the observed values and in relative proportions which do not resemble the observations either. [Al/Fe] is vice versa well fitted by three out of the four stellar models. Note that also in this case [Al/Mg] is rather small and this could be the hint that a rather large C abundance was left by the He burning in these models. The fit to the heaviest elements shows significative similarities with those shown above. Once again Sc, Ti and Co are always underproduced with respect to the observed values while Cr and Mn are always overproduced. There is however a noticeable difference in these models: [Ni/Fe] is now well fitted or even overproduced while neither our models nor those of UN02 are able to produce Ni in sufficient amount.

One could argue at this point that the failure of a good fit to the data is simply the consequence of an initial (wrong) assumption: i.e. that the observed abundances are due to just the ejecta of a single supernova event and hence that a proper choice of the mass function could modify the present analysis. Unfortunately this is not the case for the simple reason that, since no mass (within our grid) is able to provide a good fit to the three elements Ti, Cr and Ni, there is obviously no combination of masses which can fit them. A last, but not least, possibility is that all these core collapse supernovae fail to reproduce the observed abundances of the heaviest elements simply because they do not come from the ejecta of a core collapse supernova but, rather, from the ejecta of a type Ia supernova. This would not be impossible, a priori, because the typical lifetime of an intermediate mass star is not much different from that of a (low) massive star. To explore such a possibility we tried to fit the AVG star with the yields produced by a variety of Type Ia explosions published by Iwamoto et al. (1999). Figure 11 shows such a comparison; of course in this case only the fit to the heavy elements must be looked at. Also in this case no panel shows a reasonable fit to the data. It is interesting to note that also these yields miss the data systematically in the same way as the core collapse supernovae, i.e. Sc, Ti and Co are again underproduced while Cr and Mn are systematically overproduced. Ni is the only element which is rather well fitted by most of these type Ia explosive models.

5.   Conclusions

In the previous sections we have compared the ejecta of primordial core collapse supernovae with the surface chemical composition of extremely metal poor stars under the hypothesis that these stars formed in clouds enriched by just the first generation of core
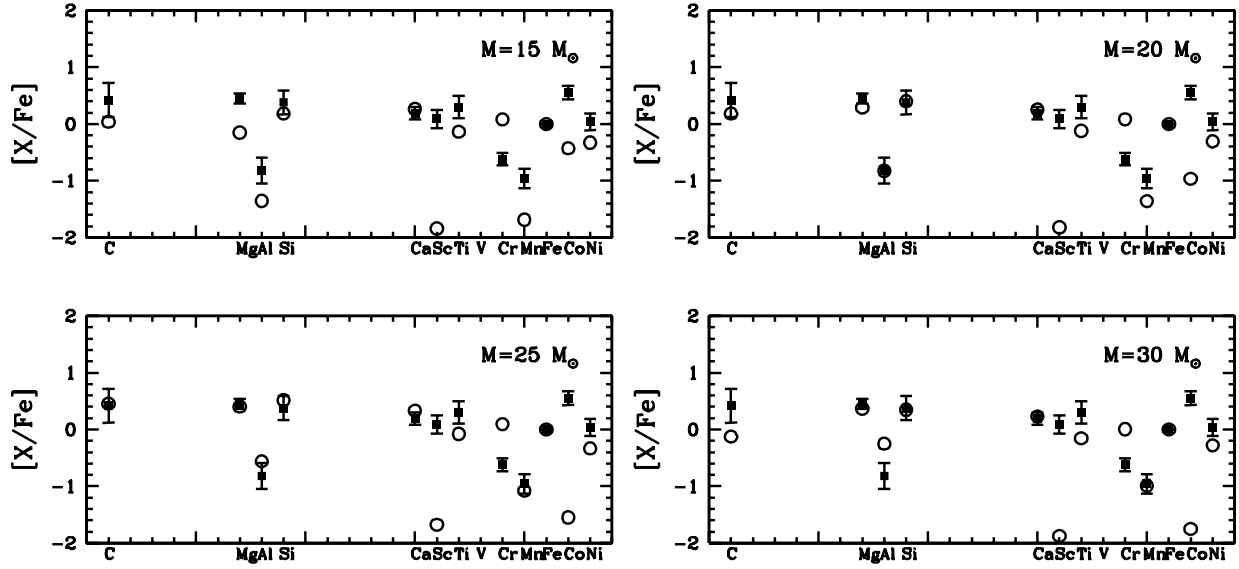
Fig. 9.— Comparison between the AVG star (*filled squares*) and the yields provided by Umeda & Nomoto (2002) (*open circles*).
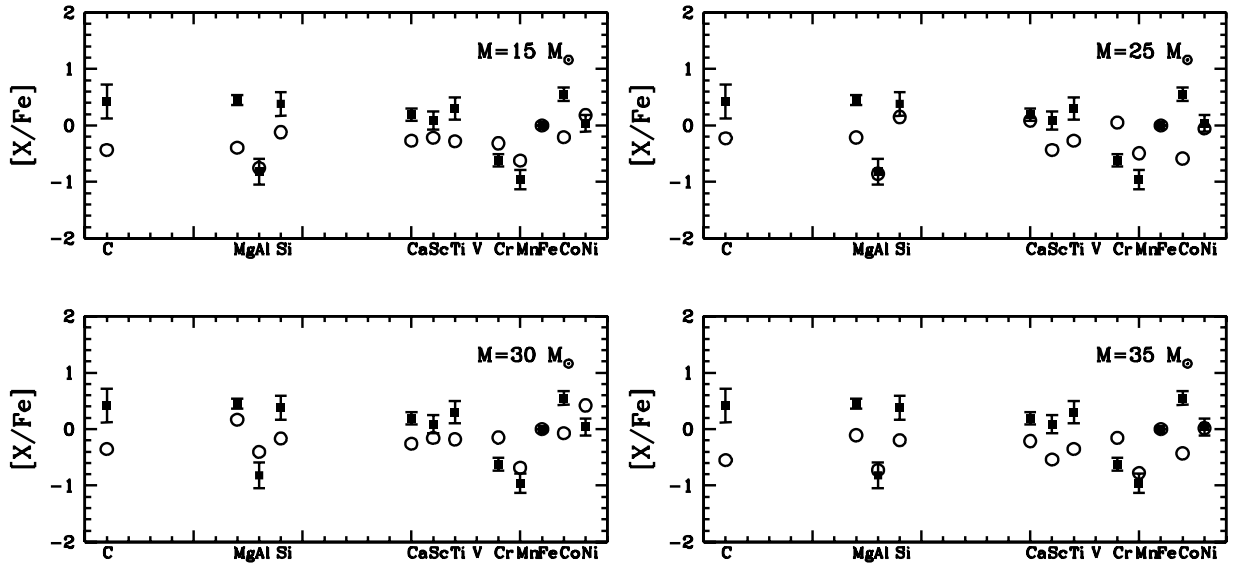

Fig. 10.— Comparison between the AVG star (*filled squares*) and the yields provided by Woosley & Weaver (1995) (*open circles*).

collapse supernovae. Such a comparison has been done with three different sets of primordial yields: ours, those published by WW95 and those recently published by UN02. The main general conclusion we feel confident to state is that none of the three sets is able to convincingly match the observed abundances. The adoption of a delta function for the mass function cannot be used as an excuse for such a defaillance. Though the three sets of yields differ significantly one from the other, all of them show embarrassing systematic similarities in missing the fit of the template star. For example, all three sets tend systematically to underproduce Ti and Ni and to overproduce Cr. Nonetheless let us stress that our models may account for more or less 2/3 of the available elements.

We have also shown above that the fit to elements like Sc and Co drastically depends on the amount of Carbon left by the He burning (see Figures 3 and 4). Such an occurrence could appear surprising because it is not so evident how the Carbon abundance may affect the relative abundances of elements produced during the explosion by the complete and incomplete explosive Si burning. Once again we refer the reader to the paper by Imbriani et al. (2001) for a comprehensive discussion of such a topic. Here let us simply remind that an increase of the Carbon abundance leads to a final mass-radius relation more flattened-out because the contraction of the ONe core is partly slowed down by the presence of a very active C-burning shell. As a consequence, the average density in the regions which will experience the complete and incomplete explosive Si burning will be lower as well. The net result is that the α rich freeze-out is considerably favored and also that the overall amount of ^{56}Ni synthesized is significantly reduced. Both these occurrences tend to increase significantly both [Sc/Fe] and [Co/Fe] (for any chosen mass cut location). In addition to that, also the yield of Mg increases with the Carbon abundance present in the He exhausted core so that, in order to maintain the ratio $\{Mg/Fe\}_{AVG}$ close to zero, the mass cut must be located more internally in order to increase also the Fe yield. It goes without saying that, since Sc and Co are mainly produced by the complete explosive Si burning, a deeper mass cut automatically tends to increase their outcome.

The strong dependence of [Co/Fe] on the carbon abundance at the end of central He burning could account for the very low [Co/Fe] obtained by other authors (Woosley & Weaver 1995; Umeda & Nomoto 2002). In fact in both computations the interplay between the treatment of convection and the adopted $^{12}C(\alpha,\gamma)^{16}O$ rate leads to a rather low carbon abundance at the end of central He burning ($X(^{12}C) \simeq 0.2$). Also Nakamura et al. (1999), who tried to explain the trend of increasing Co at low metallicities properly choosing a mass cut-initial stellar mass relation, were not able to obtain a sufficiently large [Co/Fe] ratio probably because they used models with a small carbon abundance (Nomoto & Hashimoto 1988). In order to help other groups to compare their results with the present ones we report in Table 8 for three selected zones of the 35 M$_\odot$ (set L), where we obtain a substantial
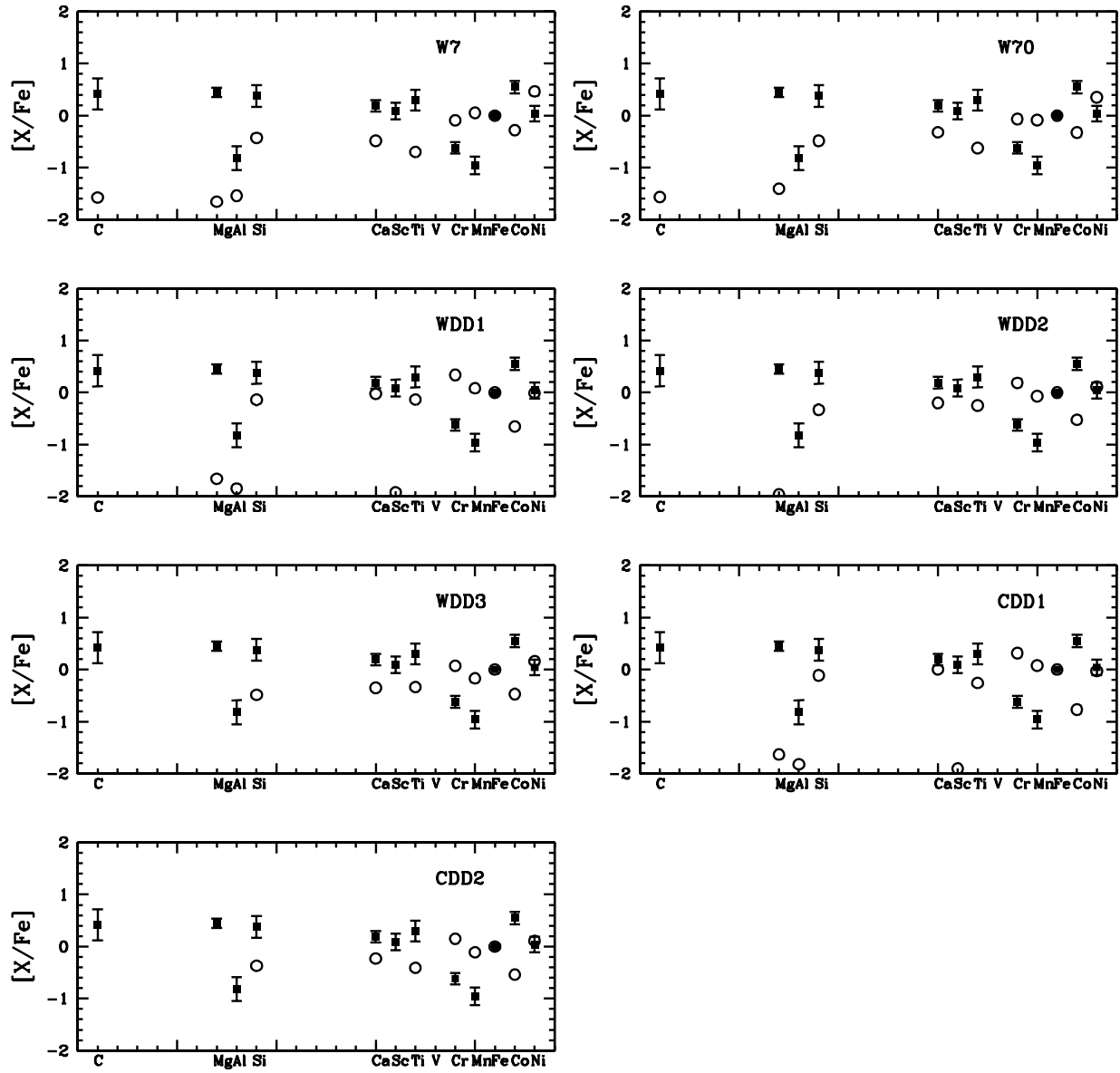
Fig. 11.— Comparison between the AVG star (*filled squares*) and the yields produced by a set of different type Ia supernovae provided by Iwamoto et al. (1999) (*open circles*).

amount of Sc and Co, the mass coordinate (column 1), the shock temperature (column 2), the shock density (column 3), the escape velocity (column 4), the electron mole fraction (column 5), the final Co and Ni mass fractions (columns 6 and 7) after the decay of all the unstable isotopes.

Very recently it has been suggested (Heger & Woosley 2002) that either an observed very low [Al/Mg] ratio as well as observed solar ratios among even elements like Si, S, Ar and Ca (e.g. [Si/Ca] $\simeq$ 0) could be a signature of a primordial generation of very massive supernovae (260 $M_\odot$ > M > 140 $M_\odot$). Though this is certainly possible, there are some points we think to be important to clarify. First of all the production (even in appreciable amounts) of odd elements like Na and Al *does not* require any neutron excess because it exists a primary sequence $^{12}C(^{12}C,p)^{23}Na(\alpha,\gamma)^{27}Al$ (where the α's also come directly from the C burning: $^{12}C(^{12}C,\alpha)^{20}Ne$) whose efficiency in producing these odd elements scales directly with the amount of C present in the He exhausted core. Figure 5 clearly shows, e.g., that an 80 $M_\odot$ with a low C abundance produces an [Al/Mg]=- 1.5 dex while a 15 $M_\odot$ with a rather large C abundance produces an [Al/Mg]=-0.5 dex. Since the amount of C left by the He burning is still subject to severe uncertainties, we think that it is not wise to use the ratio of [(light odd elements)/mg] to infer the mass function of the first stellar generation. Also the occurrence that the internal ratios among the even elements Si, S, Ar and Ca are solar (e.g. [Si/S], [Si/Ca] and the like) is not a typical property of the massive (or very massive) stars but just a property of the incomplete explosive Si burning and of the explosive Oxygen burning (also the ejecta of the thermonuclear supernovae provide these elements in roughly solar proportions). Vice versa, it is important to underline that also these ratios mildly depend on the amount of C present in the He exhausted core (Weaver & Woosley, 1993; Imbriani et al. 2001).

We want eventually stress that since each (actually most) of the elemental ratios observed in the ultra metal poor stars may be singularly reproduced, only the simultaneous fit to many (hopefully all) of the observed elemental abundances may lead to a better comprehension of the evolution and explosion of the real stars. For this reason we consider still partly unsatisfactory the fits shown in Figure 8 which miss three out of the eleven available elemental abundances.

Before closing this paper let us anticipate that we have almost completed the upgrade of the FRANEC code with the latest available cross sections for both weak processes and strong interactions and that we have extended the nuclear network up to Mo. We therefore hope to upgrade shortly also the present results and conclusions. We want also to finally stress that we barely need also homogeneous data concerning other elements like, e.g., O, K and V in order to constrain more vigorously the presupernova evolution (Oxygen) and the

explosion (Potassium and Vanadium) of the stars which provided the chemical composition of the stars we observe today.

REFERENCES

Argast, D., Samland, M., Gerhard, O.E., and Thielemann, F.K. 2000, A&A, 356, 873

Arnett, D. 1996, in Supernovae and Nucleosynthesis, Princeton University Press, p.252

Audouze, J., and Silk, J. 1995, ApJ, 451, L49

Caughlan, G.R. and Fowler, W.A., 1988, A.D.N.D.T., 40, 283

Caughlan, G.R., Fowler, W.A., Harris M.J. and Zimmerman, B.A., 1985, A.D.N.D.T., 32, 197

Chieffi, A., Limongi, M., and Straniero, O. 1998, ApJ, 502, 737

Heger, A. and Woosley, S.E. 2002, ApJ567, 532

Imbriani, G., Limongi, M. Gialanella, L., Terrasi, F., Straniero, O., Chieffi, A 2001, ApJ, 558, 903

Iwamoto, K., Brachwitz, F., Nomoto, K., Kishimoto, N., Umeda, H., Hix, R., Thielemann, F.K. 1999, ApJS, 125, 439

Limongi, M. and Chieffi, A. 2002, Publ. Astron. Soc. Aust., 19, 1

Limongi, M., Straniero, O., and Chieffi, A. 2000, ApJS, 129, 625

McWilliam, A. 1997, ARA&A, 109, 2757

McWilliam, A., Preston, G.W., Sneden, C., and Searle, L. 1995, AJ, 109, 2757

Nakamura, T., Umeda, H., Nomoto, K., Thielemann, F.K., and Burrows, A. 1999, ApJ, 517, 193

Nomoto, K., and Hashimoto, M. 1988, Phys. Rep., 256, 173

Norris, J.E., Ryan, S.G., and Beers, T.C. 2001, ApJ, 561, 1034

Ryan, S.G., Norris, J.E., and Beers, T.C. 1996, ApJ, 471, 254

Shigeyama, T. and Tsujimoto, T. 1998, ApJ, 507, L135

Thielemann, F.K., Nomoto, K., and Hashimoto, M. 1996, ApJ, 460, 408

Umeda, Nomoto, K., 2002, ApJ, 460, 408

Weaver, T.A., and Woosley. S.E. 1980, Ann. NY Acad. Sci., 336, 335

Weaver, T.A., and Woosley. S.E. 1993, Phys. Rep., 227, 65

Woosley, S.E., and Weaver, T.A. 1995, ApJS, 101, 181

Table 1.   Carbon abundance left by the central He burning

Mass($M_\odot$)	Set L	Set H
15	0.479	0.231
20	0.439	0.196
25	0.407	0.168
35	0.363	0.124
50	0.319	0.092
80	0.269	0.061

Table 2.   Explosive nucleosynthesis of the 15 M$_\odot$ Z $= 0$ model

	(1)	(2)	(3)	(4)	(5)
M(^{56}Ni)	0.0010	0.0050	0.0100	0.0500	0.0616
M$_{\mathrm{ejected}}$	1.71	1.69	1.68	1.61	1.58
M$_{\mathrm{cut}}$	13.29	13.31	13.32	13.39	13.42
H	7.74E+00	7.74E+00	7.74E+00	7.74E+00	7.74E+00
He	4.68E+00	4.68E+00	4.68E+00	4.68E+00	4.68E+00
C	1.53E-01	1.53E-01	1.53E-01	1.53E-01	1.53E-01
N	4.82E-08	4.82E-08	4.82E-08	4.82E-08	4.82E-08
O	2.34E-01	2.34E-01	2.34E-01	2.34E-01	2.34E-01
F	2.47E-10	2.47E-10	2.47E-10	2.47E-10	2.47E-10
Ne	1.05E-01	1.05E-01	1.05E-01	1.05E-01	1.05E-01
Na	1.33E-03	1.33E-03	1.33E-03	1.33E-03	1.33E-03
Mg	5.95E-02	5.95E-02	5.95E-02	5.95E-02	5.95E-02
Al	1.60E-03	1.60E-03	1.60E-03	1.60E-03	1.60E-03
Si	4.69E-02	5.51E-02	5.63E-02	5.63E-02	5.63E-02
P	1.71E-04	1.71E-04	1.71E-04	1.71E-04	1.71E-04
S	1.88E-02	2.42E-02	2.54E-02	2.54E-02	2.54E-02
Cl	5.30E-05	5.30E-05	5.30E-05	5.37E-05	5.63E-05
Ar	2.82E-03	3.89E-03	4.20E-03	4.22E-03	4.23E-03
K	1.20E-05	1.20E-05	1.20E-05	1.20E-05	1.20E-05
Ca	1.85E-03	2.85E-03	3.27E-03	3.40E-03	3.44E-03
Sc	2.80E-08	3.01E-08	3.16E-08	3.64E-07	1.78E-06
Ti	5.85E-06	2.11E-05	3.05E-05	1.28E-04	1.77E-04
V	6.92E-07	1.71E-06	2.09E-06	2.10E-06	2.10E-06
Cr	6.97E-05	3.08E-04	4.94E-04	6.44E-04	7.12E-04
Mn	3.22E-05	8.64E-05	1.17E-04	1.19E-04	1.19E-04
Fe	1.55E-03	5.93E-03	1.11E-02	5.29E-02	6.50E-02
Co	8.68E-08	9.13E-08	9.45E-08	1.43E-03	2.21E-03
Ni	4.99E-05	9.39E-05	1.30E-04	9.99E-04	1.32E-03
Cu	1.57E-13	1.57E-13	1.57E-13	1.24E-12	2.86E-12
Zn	5.12E-13	5.12E-13	5.19E-13	9.85E-08	1.87E-07

Table 3.   Explosive nucleosynthesis of the 20 $M_\odot$ $Z = 0$ model

	(1)	(2)	(3)	(4)	(5)	(6)
$M(^{56}Ni)$	0.0010	0.0050	0.0100	0.0500	0.1000	0.1406
$M_{ejected}$	2.00	1.96	1.94	1.89	1.81	1.74
M_{cut}	18.00	18.04	18.06	18.11	18.19	18.26
H	9.75E+00	9.75E+00	9.75E+00	9.75E+00	9.75E+00	9.75E+00
He	6.27E+00	6.27E+00	6.27E+00	6.27E+00	6.27E+00	6.27E+00
C	4.04E-01	4.04E-01	4.04E-01	4.04E-01	4.04E-01	4.04E-01
N	7.07E-08	7.07E-08	7.07E-08	7.07E-08	7.07E-08	7.07E-08
O	6.91E-01	6.91E-01	6.91E-01	6.91E-01	6.91E-01	6.91E-01
F	1.21E-09	1.21E-09	1.21E-09	1.21E-09	1.21E-09	1.21E-09
Ne	2.87E-01	2.87E-01	2.87E-01	2.87E-01	2.87E-01	2.87E-01
Na	3.81E-03	3.81E-03	3.81E-03	3.81E-03	3.81E-03	3.81E-03
Mg	1.31E-01	1.31E-01	1.31E-01	1.31E-01	1.31E-01	1.31E-01
Al	3.10E-03	3.10E-03	3.10E-03	3.10E-03	3.10E-03	3.10E-03
Si	9.26E-02	1.09E-01	1.15E-01	1.18E-01	1.18E-01	1.18E-01
P	3.21E-04	3.21E-04	3.21E-04	3.21E-04	3.21E-04	3.22E-04
S	3.52E-02	4.54E-02	5.01E-02	5.28E-02	5.28E-02	5.28E-02
Cl	9.17E-05	9.18E-05	9.18E-05	9.18E-05	9.21E-05	1.01E-04
Ar	5.01E-03	6.84E-03	7.89E-03	8.66E-03	8.68E-03	8.70E-03
K	2.16E-05	2.16E-05	2.17E-05	2.17E-05	2.17E-05	2.18E-05
Ca	3.18E-03	4.74E-03	5.84E-03	6.96E-03	7.06E-03	7.17E-03
Sc	5.00E-08	5.30E-08	5.51E-08	5.83E-08	1.73E-07	6.29E-06
Ti	7.68E-06	2.82E-05	4.77E-05	8.73E-05	1.81E-04	2.95E-04
V	9.65E-07	2.54E-06	3.57E-06	4.99E-06	4.99E-06	4.99E-06
Cr	8.08E-05	3.66E-04	6.69E-04	1.35E-03	1.48E-03	1.64E-03
Mn	4.01E-05	1.10E-04	1.65E-04	2.78E-04	2.78E-04	2.78E-04
Fe	1.83E-03	6.40E-03	1.17E-02	5.30E-02	1.05E-01	1.47E-01
Co	1.38E-07	1.43E-07	1.46E-07	2.21E-04	1.28E-03	2.24E-03
Ni	6.56E-05	1.14E-04	1.48E-04	4.34E-04	8.67E-04	1.99E-03
Cu	2.11E-13	2.11E-13	2.11E-13	2.18E-13	4.50E-13	1.17E-12
Zn	7.10E-13	7.11E-13	7.11E-13	4.13E-09	5.17E-08	1.45E-07

Table 4.   Explosive nucleosynthesis of the 25 M$_\odot$ Z $= 0$ model

	(1)	(2)	(3)	(4)
M(^{56}Ni)	0.0010	0.0050	0.0100	0.0313
M$_{\mathrm{ejected}}$	1.66	1.63	1.63	1.57
M$_{\mathrm{cut}}$	23.34	23.37	23.37	23.43
H	1.15E+01	1.15E+01	1.15E+01	1.15E+01
He	7.86E+00	7.86E+00	7.86E+00	7.86E+00
C	5.49E-01	5.49E-01	5.49E-01	5.49E-01
N	6.89E-08	6.89E-08	6.89E-08	6.89E-08
O	1.51E+00	1.51E+00	1.51E+00	1.51E+00
F	3.47E-09	3.47E-09	3.47E-09	3.47E-09
Ne	1.15E+00	1.15E+00	1.15E+00	1.15E+00
Na	9.63E-03	9.63E-03	9.63E-03	9.63E-03
Mg	2.85E-01	2.85E-01	2.85E-01	2.85E-01
Al	6.91E-03	6.91E-03	6.91E-03	6.91E-03
Si	5.67E-02	6.59E-02	6.72E-02	6.73E-02
P	1.49E-04	1.49E-04	1.49E-04	1.49E-04
S	1.65E-02	2.25E-02	2.37E-02	2.39E-02
Cl	3.61E-05	3.61E-05	3.61E-05	4.17E-05
Ar	2.55E-03	3.68E-03	4.04E-03	4.12E-03
K	7.28E-06	7.29E-06	7.30E-06	7.34E-06
Ca	1.97E-03	2.99E-03	3.47E-03	3.69E-03
Sc	2.23E-08	2.41E-08	2.52E-08	3.08E-06
Ti	4.66E-06	1.94E-05	2.98E-05	1.04E-04
V	3.14E-07	8.96E-07	1.10E-06	1.14E-06
Cr	5.48E-05	2.82E-04	4.90E-04	6.85E-04
Mn	1.89E-05	5.26E-05	6.94E-05	7.48E-05
Fe	1.23E-03	5.42E-03	1.05E-02	3.23E-02
Co	3.50E-08	3.77E-08	3.89E-08	1.29E-03
Ni	3.18E-05	6.67E-05	9.17E-05	5.59E-04
Cu	2.87E-14	2.87E-14	2.87E-14	1.64E-11
Zn	1.29E-13	1.29E-13	1.29E-13	1.82E-07

Table 5.   Explosive nucleosynthesis of the 35 M$_\odot$ Z $= 0$ model

	(1)	(2)	(3)	(4)	(5)	(6)	(7)	(8)
M(^{56}Ni)	0.0010	0.0050	0.0100	0.0500	0.1000	0.1500	0.2000	0.2500
M$_{ejected}$	2.55	2.48	2.43	2.33	2.28	2.21	2.15	2.08
M$_{cut}$	32.45	32.52	32.57	32.67	32.72	32.79	32.85	32.92
H	1.47E+01	1.47E+01	1.47E+01	1.47E+01	1.47E+01	1.47E+01	1.47E+01	1.47E+01
He	1.07E+01	1.07E+01	1.07E+01	1.07E+01	1.07E+01	1.07E+01	1.07E+01	1.07E+01
C	1.23E+00	1.23E+00	1.23E+00	1.23E+00	1.23E+00	1.23E+00	1.23E+00	1.23E+00
N	2.24E-04	2.24E-04	2.24E-04	2.24E-04	2.24E-04	2.24E-04	2.24E-04	2.24E-04
O	3.57E+00	3.57E+00	3.57E+00	3.57E+00	3.57E+00	3.57E+00	3.57E+00	3.57E+00
F	6.39E-07	6.39E-07	6.39E-07	6.39E-07	6.39E-07	6.39E-07	6.39E-07	6.39E-07
Ne	9.45E-01	9.45E-01	9.45E-01	9.45E-01	9.45E-01	9.45E-01	9.45E-01	9.45E-01
Na	9.75E-03	9.75E-03	9.75E-03	9.75E-03	9.75E-03	9.75E-03	9.75E-03	9.75E-03
Mg	3.49E-01	3.49E-01	3.49E-01	3.49E-01	3.49E-01	3.49E-01	3.49E-01	3.49E-01
Al	5.13E-03	5.13E-03	5.13E-03	5.13E-03	5.13E-03	5.13E-03	5.13E-03	5.13E-03
Si	2.11E-01	2.45E-01	2.69E-01	2.94E-01	2.95E-01	2.95E-01	2.95E-01	2.95E-01
P	5.59E-04	5.59E-04	5.59E-04	5.60E-04	5.60E-04	5.60E-04	5.60E-04	5.60E-04
S	6.67E-02	8.60E-02	1.01E-01	1.21E-01	1.22E-01	1.22E-01	1.22E-01	1.22E-01
Cl	1.22E-04	1.23E-04	1.23E-04	1.23E-04	1.23E-04	1.23E-04	1.23E-04	1.23E-04
Ar	8.52E-03	1.18E-02	1.44E-02	1.93E-02	1.97E-02	1.97E-02	1.98E-02	1.98E-02
K	3.23E-05	3.24E-05	3.25E-05	3.25E-05	3.25E-05	3.25E-05	3.25E-05	3.25E-05
Ca	5.61E-03	8.25E-03	1.05E-02	1.60E-02	1.68E-02	1.68E-02	1.69E-02	1.69E-02
Sc	7.65E-08	8.11E-08	8.45E-08	9.29E-08	1.02E-07	1.28E-07	1.51E-07	2.83E-07
Ti	8.65E-06	3.24E-05	6.00E-05	1.77E-04	2.16E-04	2.56E-04	3.10E-04	3.77E-04
V	1.07E-06	2.91E-06	4.60E-06	8.54E-06	9.45E-06	9.45E-06	9.45E-06	9.45E-06
Cr	8.57E-05	3.91E-04	7.59E-04	2.84E-03	3.67E-03	3.72E-03	3.80E-03	3.89E-03
Mn	4.38E-05	1.20E-04	1.93E-04	4.31E-04	5.16E-04	5.16E-04	5.16E-04	5.16E-04
Fe	2.01E-03	6.70E-03	1.22E-02	5.33E-02	1.04E-01	1.56E-01	2.07E-01	2.59E-01
Co	1.46E-07	1.51E-07	1.55E-07	1.61E-07	1.47E-04	4.82E-04	9.84E-04	1.58E-03
Ni	7.57E-05	1.27E-04	1.70E-04	2.87E-04	4.41E-04	6.67E-04	8.73E-04	1.21E-03
Cu	3.14E-11	3.14E-11	3.14E-11	3.14E-11	3.14E-11	3.14E-11	3.14E-11	3.15E-11
Zn	9.83E-10	9.83E-10	9.83E-10	9.83E-10	2.93E-09	1.11E-08	2.54E-08	4.65E-08

Table 6.   Explosive nucleosynthesis of the 50 M$_\odot$ Z $= 0$ model

	(1)	(2)	(3)	(4)	(5)	(6)	(7)	(8)
M(^{56}Ni)	0.0010	0.0050	0.0100	0.0500	0.1000	0.1500	0.2000	0.2500
M$_{ejected}$	2.61	2.55	2.50	2.39	2.34	2.28	2.21	2.14
M$_{cut}$	47.39	47.45	47.50	47.61	47.66	47.72	47.79	47.86
H	1.94E+01	1.94E+01	1.94E+01	1.94E+01	1.94E+01	1.94E+01	1.94E+01	1.94E+01
He	1.53E+01	1.53E+01	1.53E+01	1.53E+01	1.53E+01	1.53E+01	1.53E+01	1.53E+01
C	2.51E+00	2.51E+00	2.51E+00	2.51E+00	2.51E+00	2.51E+00	2.51E+00	2.51E+00
N	1.12E-06	1.12E-06	1.12E-06	1.12E-06	1.12E-06	1.12E-06	1.12E-06	1.12E-06
O	6.88E+00	6.88E+00	6.88E+00	6.88E+00	6.88E+00	6.88E+00	6.88E+00	6.88E+00
F	4.33E-09	4.33E-09	4.33E-09	4.33E-09	4.33E-09	4.33E-09	4.33E-09	4.33E-09
Ne	2.01E+00	2.01E+00	2.01E+00	2.01E+00	2.01E+00	2.01E+00	2.01E+00	2.01E+00
Na	1.07E-02	1.07E-02	1.07E-02	1.07E-02	1.07E-02	1.07E-02	1.07E-02	1.07E-02
Mg	3.26E-01	3.26E-01	3.26E-01	3.26E-01	3.26E-01	3.26E-01	3.26E-01	3.26E-01
Al	3.69E-03	3.69E-03	3.69E-03	3.69E-03	3.69E-03	3.69E-03	3.69E-03	3.69E-03
Si	1.55E-01	1.84E-01	2.08E-01	2.37E-01	2.37E-01	2.37E-01	2.37E-01	2.37E-01
P	1.60E-04	1.60E-04	1.60E-04	1.61E-04	1.61E-04	1.61E-04	1.61E-04	1.61E-04
S	5.79E-02	7.59E-02	9.03E-02	1.13E-01	1.13E-01	1.13E-01	1.13E-01	1.13E-01
Cl	6.82E-05	6.83E-05	6.84E-05	6.85E-05	6.86E-05	6.87E-05	6.90E-05	7.00E-05
Ar	8.77E-03	1.20E-02	1.46E-02	1.97E-02	2.00E-02	2.00E-02	2.00E-02	2.00E-02
K	2.92E-05	2.93E-05	2.93E-05	2.94E-05	2.94E-05	2.94E-05	2.94E-05	2.94E-05
Ca	6.35E-03	9.15E-03	1.13E-02	1.70E-02	1.76E-02	1.77E-02	1.77E-02	1.78E-02
Sc	8.58E-08	9.05E-08	9.36E-08	1.02E-07	1.20E-07	1.91E-07	3.21E-07	7.88E-07
Ti	8.45E-06	3.07E-05	5.77E-05	1.73E-04	2.05E-04	2.52E-04	3.12E-04	3.86E-04
V	7.87E-07	2.15E-06	3.57E-06	7.36E-06	8.00E-06	8.00E-06	8.00E-06	8.00E-06
Cr	7.42E-05	3.59E-04	7.19E-04	2.77E-03	3.46E-03	3.53E-03	3.61E-03	3.71E-03
Mn	3.54E-05	9.71E-05	1.61E-04	3.89E-04	4.64E-04	4.64E-04	4.64E-04	4.64E-04
Fe	1.73E-03	6.22E-03	1.16E-02	5.27E-02	1.04E-01	1.55E-01	2.06E-01	2.58E-01
Co	1.21E-07	1.25E-07	1.28E-07	1.34E-07	1.33E-04	4.65E-04	8.63E-04	1.37E-03
Ni	6.31E-05	1.05E-04	1.42E-04	2.64E-04	4.67E-04	8.05E-04	1.23E-03	1.82E-03
Cu	9.41E-14	9.41E-14	9.41E-14	9.41E-14	9.54E-14	1.07E-13	1.28E-13	1.77E-13
Zn	4.12E-13	4.12E-13	4.12E-13	4.12E-13	1.90E-09	1.14E-08	2.52E-08	4.72E-08

Table 7. Explosive nucleosynthesis of the 80 M$_\odot$ Z $= 0$ model

	(1)	(2)	(3)	(4)	(5)	(6)	(7)	(8)
M(^{56}Ni)	0.0010	0.0050	0.0100	0.0500	0.1000	0.1500	0.2000	0.2500
M$_{\rm ejected}$	3.80	3.72	3.65	3.42	3.32	3.25	3.20	3.14
M$_{\rm cut}$	76.20	76.28	76.35	76.58	76.68	76.75	76.80	76.86
H	2.68E+01	2.68E+01	2.68E+01	2.68E+01	2.68E+01	2.68E+01	2.68E+01	2.68E+01
He	2.47E+01	2.47E+01	2.47E+01	2.47E+01	2.47E+01	2.47E+01	2.47E+01	2.47E+01
C	4.67E+00	4.67E+00	4.67E+00	4.67E+00	4.67E+00	4.67E+00	4.67E+00	4.67E+00
N	1.98E-06	1.98E-06	1.98E-06	1.98E-06	1.98E-06	1.98E-06	1.98E-06	1.98E-06
O	1.50E+01	1.50E+01	1.50E+01	1.50E+01	1.50E+01	1.50E+01	1.50E+01	1.50E+01
F	4.09E-09	4.09E-09	4.09E-09	4.09E-09	4.09E-09	4.09E-09	4.09E-09	4.09E-09
Ne	2.63E+00	2.63E+00	2.63E+00	2.63E+00	2.63E+00	2.63E+00	2.63E+00	2.63E+00
Na	7.62E-03	7.62E-03	7.62E-03	7.62E-03	7.62E-03	7.62E-03	7.62E-03	7.62E-03
Mg	6.04E-01	6.04E-01	6.04E-01	6.04E-01	6.04E-01	6.04E-01	6.04E-01	6.04E-01
Al	3.19E-03	3.19E-03	3.19E-03	3.19E-03	3.19E-03	3.19E-03	3.19E-03	3.19E-03
Si	3.35E-01	3.75E-01	4.07E-01	5.05E-01	5.24E-01	5.28E-01	5.28E-01	5.28E-01
P	6.47E-04	6.47E-04	6.47E-04	6.48E-04	6.49E-04	6.49E-04	6.49E-04	6.49E-04
S	1.16E-01	1.42E-01	1.61E-01	2.28E-01	2.46E-01	2.51E-01	2.51E-01	2.51E-01
Cl	1.46E-04	1.46E-04	1.46E-04	1.46E-04	1.46E-04	1.46E-04	1.46E-04	1.47E-04
Ar	1.60E-02	2.09E-02	2.41E-02	3.74E-02	4.21E-02	4.37E-02	4.39E-02	4.39E-02
K	5.86E-05	5.87E-05	5.87E-05	5.89E-05	5.89E-05	5.89E-05	5.89E-05	5.89E-05
Ca	1.17E-02	1.61E-02	1.87E-02	3.13E-02	3.72E-02	3.96E-02	4.00E-02	4.00E-02
Sc	1.69E-07	1.77E-07	1.80E-07	1.95E-07	2.03E-07	2.07E-07	2.22E-07	2.85E-07
Ti	1.11E-05	3.34E-05	6.12E-05	2.40E-04	3.77E-04	4.62E-04	4.84E-04	5.09E-04
V	9.90E-07	2.38E-06	3.82E-06	1.04E-05	1.37E-05	1.56E-05	1.60E-05	1.60E-05
Cr	8.14E-05	3.52E-04	7.15E-04	3.31E-03	5.84E-03	7.85E-03	8.31E-03	8.34E-03
Mn	4.37E-05	1.10E-04	1.74E-04	5.03E-04	7.17E-04	8.80E-04	9.20E-04	9.20E-04
Fe	2.13E-03	6.70E-03	1.22E-02	5.39E-02	1.05E-01	1.55E-01	2.06E-01	2.57E-01
Co	2.05E-07	2.11E-07	2.14E-07	2.24E-07	2.28E-07	2.30E-07	1.18E-04	2.97E-04
Ni	9.57E-05	1.47E-04	1.86E-04	3.61E-04	4.60E-04	5.38E-04	7.45E-04	1.03E-03
Cu	1.32E-13	1.32E-13	1.32E-13	1.32E-13	1.32E-13	1.32E-13	1.32E-13	1.34E-13
Zn	6.26E-13	6.26E-13	6.26E-13	6.27E-13	6.27E-13	6.27E-13	1.38E-09	5.15E-09

Table 8.   Selected quantities of three mass coordinates of the exploded 35 M$_\odot$ model (set L)

Mass coordinate (M$_\odot$)	T_{shock} (K)	ρ_{shock} (g/cm^3)	v_{escape} (Km/s)	Y_{e}	Co	Sc
2.01	9.53(9)	1.02(7)	1.52(4)	0.499696	1.42(-3)	2.81(-4)
2.07	7.67(9)	6.80(6)	1.38(4)	0.499697	8.61(-3)	5.84(-6)
2.30	5.13(9)	2.89(6)	1.12(4)	0.499775	4.70(-3)	9.66(-8)